

Magnetic anisotropy of Fe and Co adatoms and monolayers: Need for a proper treatment of the substrate

O. Šipr,^{1,*} S. Bornemann,² J. Minár,² and H. Ebert^{2,†}

¹*Institute of Physics AS CR, v. v. i., Cukrovarnická 10, CZ-162 53 Prague, Czech Republic*

²*Department Chemie und Biochemie, Universität München, Butenandtstr. 5-13, D-81377 München, Germany*

(Received 18 August 2010; published 10 November 2010)

The magnetocrystalline contribution to the magnetic anisotropy energy (MAE) of Fe and Co adatoms, monolayers, and surface superstructures on Pt(111) is investigated. It is shown that the thickness of the slab representing the substrate and the interaction between the atoms in neighboring surface supercells affect the calculated MAE much more profoundly than they affect magnetic moments. Reliable theoretical values of MAE cannot be obtained if the substrate is represented by a slab of less than about ten atomic layers. If a surface superstructure is meant to represent an adatom by means of supercell approach, then decoupling has to be ensured by using very large supercells.

DOI: [10.1103/PhysRevB.82.174414](https://doi.org/10.1103/PhysRevB.82.174414)

PACS number(s): 75.30.Gw, 75.70.Ak, 75.75.Lf, 75.10.Lp

I. INTRODUCTION

Magnetism of clusters and monolayers exhibits larger variability than magnetism of their bulk counterparts: small variations in size, shape, and composition may lead to large changes in their magnetic properties. One of the key issues in exploiting this in technical applications is the direction of magnetization with respect to the atomic structure. Understanding various aspects of magnetic anisotropy of nanostructures is thus of fundamental importance.

Sophisticated experiments were used in the past to measure the magnetic anisotropy of monolayers or even individual adatoms. In particular, this is the case of Fe and Co on the Pt(111) surface.¹⁻³ Obviously, there is a need to supplement these experiments with theory. On one hand, calculations can elucidate the mechanism behind the extraordinary large magnetic anisotropy [such as the spin-orbit coupling (SOC) in the nonmagnetic substrate]. On the other hand, calculations are needed to confirm the results of experiments as those are themselves very challenging and sometimes not easy to interpret.

To calculate the magnetic anisotropy energy (MAE), one has to evaluate the difference between total energies of a magnetic material for different orientations of the magnetization \mathbf{M} . This is numerically a very demanding task and it remains challenging even if the need to directly subtract total energies is bypassed. Calculating the MAE of atoms, clusters, and monolayers is difficult also because band-structure methods cannot be straightforwardly applied to these systems due to the lack of translational periodicity; one has to rely on supercells if well-established bulk system techniques are to be used.

Several calculations of the MAE of zero-, one-, and two-dimensional transition-metal systems supported by noble metal surfaces were done in the past. The research focused on several aspects, such as the role of the substrate,^{2,4} geometry relaxation,^{2,5,6} alloying,² cluster size,^{1,7} and many-body effects beyond the local spin-density approximation (LSDA).^{1,6,8,9} The agreement with experiment was usually not very good, with deviations of tens of percent or more.^{1,3,6,10}

There are several possible sources of errors in MAE calculations. An obvious one is the need to compromise between numerical accuracy and computational effort. For example, the convergence of the MAE with respect to the number of the \mathbf{k}_{\parallel} points used in obtaining the self-consistent potential and in evaluating the band or total energies is important.^{11,12} There may be similar issues connected with the energy cutoff of the plane waves (and also with construction of the pseudopotentials).^{13,14}

Another problem is many-body effects beyond the LSDA. The orbital magnetic moment μ_{orb} of $3d$ transition metals and of their impurities and their alloys with noble metals can be calculated correctly only if correlations are included, e.g., via a combination of the LSDA and the dynamical mean-field theory (LSDA+DMFT).^{15,16} As orbital magnetism and the MAE are governed by similar mechanisms, insufficiency of the LSDA to yield correct values of μ_{orb} suggests its insufficiency to yield correct values of the MAE as well. Indeed, for adatoms, large changes in the MAE caused by including the orbital polarization term of Brooks or by going from the LSDA to the generalized gradient approximation were observed.^{6,8} As concerns bulk alloys, the role of correlations on the MAE of CoPt and FePt was investigated via the LSDA+ U method.¹⁷

The theoretical investigations done so far indicate that calculations of the MAE with an accuracy necessary to aspire to a favorable comparison with experiment have to include structural relaxations and many-body effects (apart from the obvious but nontrivial issue of numerical soundness). However, there is yet another aspect that has hardly been addressed so far. Namely, in most calculations of the MAE of adsorbed systems, a semi-infinite substrate is represented by a slab of only a few atomic layers and an isolated adatom is substituted by a periodic array of atoms located at grid points of a surface supercell.^{5,6,10} This simplification usually has only a small effect on magnetic moments. However, the MAE is a much more sensitive quantity. It is conceivable that a simplified treatment of the substrate or the neglect of the zero-dimensional character of adatoms could have significant influence. Exploring systematically how the calculated MAE depends on the thickness of the slab repre-

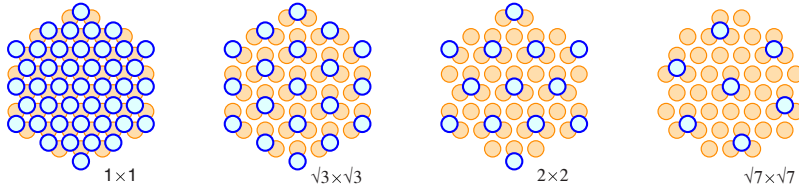


FIG. 1. (Color online) Top view of 1×1 , $\sqrt{3} \times \sqrt{3}$, 2×2 , and $\sqrt{7} \times \sqrt{7}$ surface superstructures on Pt(111).

senting the substrate and on the size of the surface supercell approximating the isolated adatom is thus desirable. Such a study might have implications for experiments as well because it would suggest for which concentrations the adatoms cannot be regarded as independent any more.

As a case study, we investigate the MAE of Fe and Co on Pt(111). We will show that thickness of the slab representing the substrate and the interaction between the adatoms affect the calculated values of the MAE much more profoundly than they affect calculated values of magnetic moments. Without a proper treatment of the substrate and a very low concentration of the adatoms, no calculation can aspire to a good quantitative agreement with experiment.

II. COMPUTATIONAL SCHEME

The calculations were performed within the *ab initio* spin-density-functional framework, relying on the LSDA. The Vosko *et al.*¹⁸ parametrization of the exchange and correlation potential was used. The electronic structure is described, including all relativistic effects, by the Dirac equation, which is solved using the spin-polarized relativistic multiple-scattering or Korringa-Kohn-Rostoker (KKR) formalism.^{19,20} The electronic structure of two-dimensional systems (slabs) was calculated by means of the tight-binding or screened KKR technique.²¹ Semi-infinite systems were dealt with by means of the decimation technique.²²

Adatoms were treated as embedded impurities, by solving self-consistently the Dyson equation^{23,24} for an impurity cluster of 50–80 sites embedded in a host. Spurious interaction between adatoms, which may be present if adatoms are treated via a surface supercell calculation, is thus avoided and yet the whole system is formally infinite.

Only the magnetocrystalline contribution to the MAE is considered here. We rely on the magnetic force theorem to calculate it. Technically, this is performed by evaluating the torque $T_{\hat{u}}^{(\hat{n})}$, which describes the variation in the energy if the magnetization direction \hat{n} is infinitesimally rotated around an axis \hat{u} . By using the magnetic force theorem, Lloyd's formula and perturbation theory, $T_{\hat{u}}^{(\hat{n})}$ can be expressed as²⁵

$$T_{\hat{u}}^{(\hat{n})} = -\frac{1}{\pi} \text{Im} \int_{-\infty}^{E_F} dE \sum_i \text{Tr}(\underline{t}_{ii}^{(\hat{n})} [(\hat{u} \cdot \hat{J}) \underline{t}_i^{(\hat{n})-1} - \underline{t}_i^{(\hat{n})-1} (\hat{u} \cdot \hat{J})]). \quad (1)$$

Here \hat{J} is the total angular momentum operator and the matrices $\underline{t}_i^{(\hat{n})}$ and $\underline{t}_{ii}^{(\hat{n})}$ are the single site t -matrix and the site diagonal scattering path operator and i labels atomic sites. Formally, the magnetic anisotropy energy, defined as the difference $E(\hat{n}, \hat{n}_0)$ of the energy for two orientations of the

magnetization \hat{n} and \hat{n}_0 , has to be determined by a corresponding path integral

$$E(\hat{n}, \hat{n}_0) = \int_{\hat{n}_0}^{\hat{n}} T^{(\hat{n})} d\hat{n}. \quad (2)$$

However, if the system is uniaxial so that the total energy can be approximated by

$$E(\theta) = E_0 + K_2 \sin^2(\theta) + K_4 \sin^4(\theta), \quad (3)$$

the difference $E(90^\circ) - E(0^\circ)$ is equal to the torque evaluated for $\theta = 45^\circ$.²⁶ Thus, instead of subtracting band or total energies, we perform a self-consistent calculation with the magnetization tilted by an angle of 45° and sum the torque moments [Eq. (1)] exerted on each atom.

To check the stability of our procedure, we evaluated the MAE additionally also by two other approaches for several systems, namely, by evaluating the difference in the band energies (again relying on the magnetic force theorem) and by subtracting the total energies. We found a good agreement between all the methods: the differences in the MAE calculated by different approaches were typically about 5%.

Integration over the surface Brillouin zones (BZs) was done using a regular mesh of 80×80 \mathbf{k}_{\parallel} points, which amounts to 1107 points in the irreducible part of the BZ if the magnetization is oriented perpendicular to the surface. We used this grid both for self-consistent calculations as well as for the evaluation of the magnetic torque. For supercell calculations ($\sqrt{3} \times \sqrt{3}$, 2×2 , and $\sqrt{7} \times \sqrt{7}$ surface superstructures), the number of the \mathbf{k}_{\parallel} points was scaled down proportionally so that their density is maintained.

The potentials were treated within the atomic sphere approximation and for the multipole expansion of the Green's function, an angular momentum cutoff $\ell_{\max} = 2$ was used. These restrictions may limit the accuracy of the resulting MAE but in any case do not hinder the investigation of the dependency of the MAE on the thickness of the substrate slab or on the size of the surface supercell.

III. INVESTIGATED SYSTEMS

We focus on Fe and Co adatoms, monolayers and $\sqrt{3} \times \sqrt{3}$, 2×2 , and $\sqrt{7} \times \sqrt{7}$ surface superstructures on a Pt(111) surface (see Fig. 1). The substrate is usually represented by a finite slab; if not stated otherwise, the slab comprises $n_{\text{Pt}} = 10$ platinum layers. Few comparative calculations were done also for a semi-infinite Pt crystal. The structure of the substrate was taken as of bulk Pt (fcc lattice constant 3.91 Å). The vacuum is represented by layers of empty sites, a spill-over of electrons into three such vacuum layers is allowed.

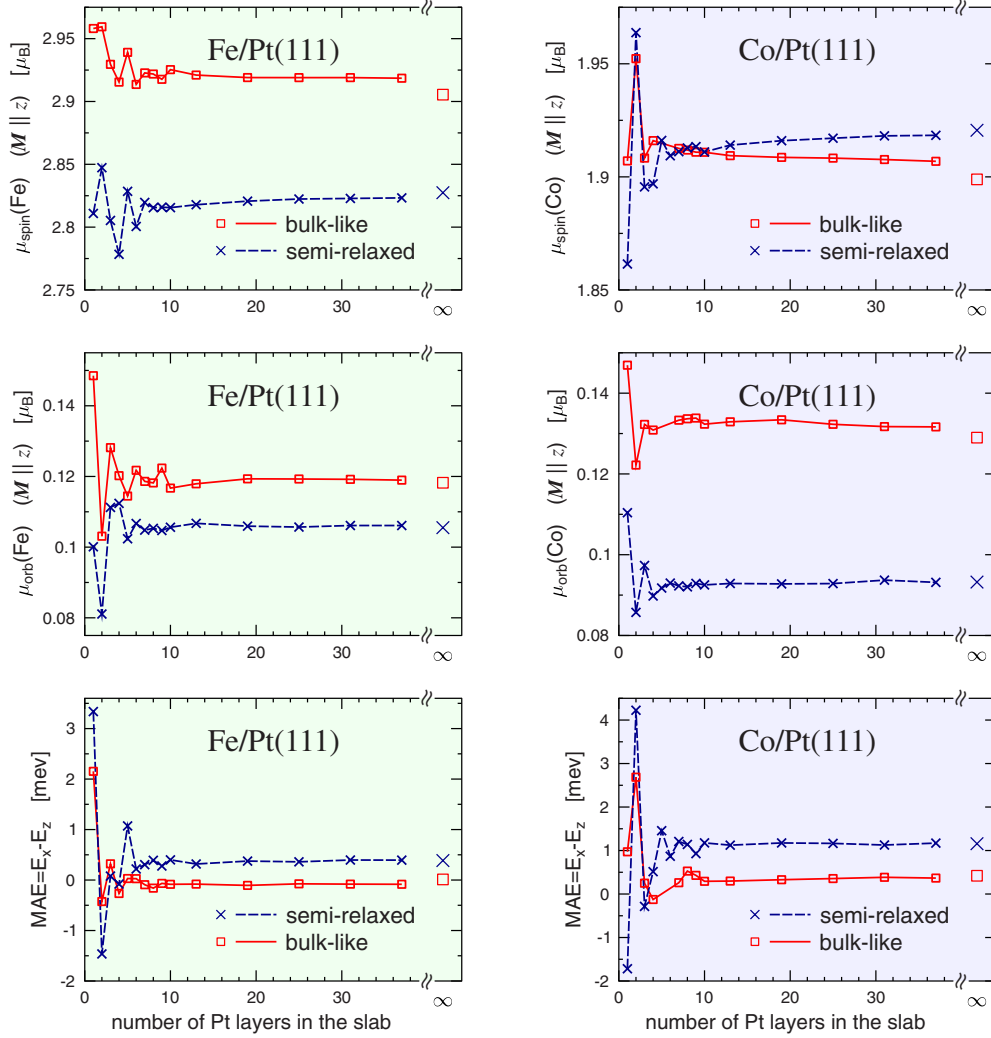


FIG. 2. (Color online) Calculated magnetic moments and the MAE of full Fe (left panels) and Co (right panels) monolayers on Pt(111) with bulklike and semirelaxed structures for different thicknesses of the substrate slab. Magnetic moments inside the Fe or Co spheres obtained for magnetization perpendicular to the surface are shown in the upper panels (μ_{spin}) and in the middle panels (μ_{orb}). The lowermost panels display the MAE. Values for semi-infinite substrate are shown via markers close to the right edges of the panels.

As concerns the distance between Fe or Co layers and Pt layers, we investigated two series of systems: (i) nonrelaxed structure, with Fe/Co-Pt interlayer distance taken as in bulk Pt ($z_{\text{Fe/Co-Pt}}=2.26$ Å) and (ii) semirelaxed structure, with Fe/Co-Pt interlayer distances estimated from earlier calculations as $z_{\text{Fe-Pt}}=1.82$ Å and $z_{\text{Co-Pt}}=1.80$ Å. These semirelaxed distances were taken identical for all the Fe/Co coverages and fall between the interlayer distances for adatoms (1.65–1.70 Å) (Refs. 3, 6, and 27) and complete monolayers (1.95–2.05 Å).^{10,28–30} The small difference between our $z_{\text{Fe-Pt}}$ and $z_{\text{Co-Pt}}$ distances reflects somewhat different atomic volumes of Fe and Co.

IV. RESULTS AND DISCUSSION

A. Dependence of magnetic moments and the MAE on the thickness of the slab

We begin by focusing on full Fe and Co monolayers on Pt(111) substrate, which is represented by a slab of 1–37 Pt

layers or by a semi-infinite crystal. We calculated magnetic moments and the MAE defined as the energy difference $E_x - E_z$, with $E_{x(z)}$ being the energy for the magnetization along the x (z) direction and z being the surface normal. The results for both bulklike and semirelaxed structures are shown in Fig. 2.

One can see that μ_{spin} , μ_{orb} , and the MAE are very sensitive to the Pt slab thickness for $n_{\text{Pt}} \lesssim 10$. A closer inspection of the amplitudes of the quasioscillations reveals that the situation is different for μ_{spin} and μ_{orb} on the one side and the MAE on the other side. The variations in μ_{spin} with n_{Pt} do not exceed 2% of the value and the variations in μ_{orb} do not exceed 10% (if we exclude the extreme cases of $n_{\text{Pt}}=1$ or 2). Quantitatively accurate estimates of μ_{spin} and μ_{orb} thus can be made even for relatively thin Pt slabs. Analogous variations in the MAE, however, can amount to 50% or more (cf. the numbers on the vertical axes of the lowermost graphs in Fig. 2). Consequently, for studying the MAE, sufficiently thick slabs of at least seven to ten Pt layers should be used to ensure convergence.

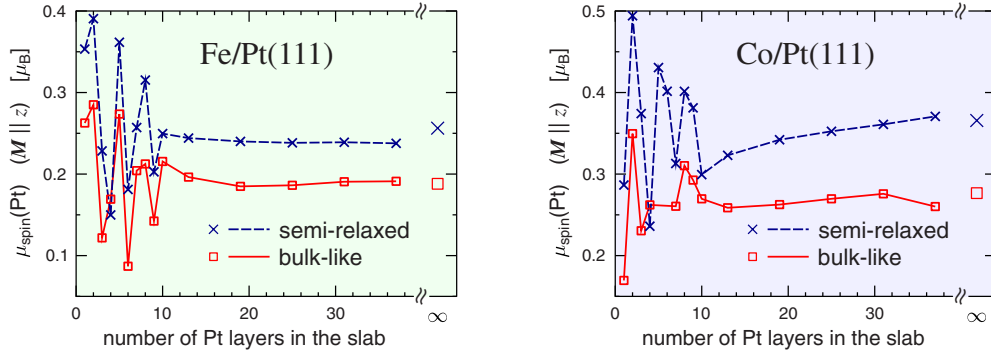


FIG. 3. (Color online) Calculated μ_{spin} induced in the Pt substrate for Fe (left panels) and Co (right panels) monolayers on Pt(111). The values of $\mu_{\text{spin}}(\text{Pt})$ refer to a sum of contributions of all substrate layers and are related to one Fe or Co atom. This figure is analogous to Fig. 2.

The magnetic moments given in Fig. 2 represent the Fe and Co spheres only. In systems containing nonmagnetic elements with a high polarizability such as V, Pd, or Pt, induced moments can be appreciable, with important consequences for the MAE. Therefore, the total μ_{spin} induced in the Pt substrate is shown as a function of the Pt slab thickness in Fig. 3. Similarly to the MAE, oscillations with quite large amplitude appear for less than about ten Pt layers.

Large induced magnetic moments in the Pt substrate are probably the reason why the MAE depends on the substrate slab thickness even for relatively large n_{Pt} . We do not expect similar sensitivity to the slab thickness for substrates with low polarizability, such as Cu or Au.

The magnetic moments and MAE obtained for a semi-infinite substrate do not always perfectly match the perceived $n_{\text{Pt}} \rightarrow \infty$ limit in Figs. 2 and 3. There is a technical reason for this. The $n_{\text{Pt}} \rightarrow \infty$ sequence, namely, gradually approaches an infinitely thick slab in such a way that the electronic structure is relaxed in each of its layers. On the other hand, when dealing with semi-infinite crystals, the electronic structure is allowed to relax to the presence of the surface only in a finite number of layers (eight in our case) and then it is matched to the electronic structure of the bulk.

To summarize this section, the strong and nonmonotonous dependence of the MAE on the thickness of the Pt slab for $n_{\text{Pt}} \lesssim 10$ implies that reliable values of the MAE of adsorbed systems cannot be obtained if the substrate is represented by a slab of only four to five layers.^{5,6,10,31} The same applies to magnetic moments induced in the nonmagnetic substrate.⁶

Bloch spectral function of a finite slab and of a semi-infinite crystal

So far we have investigated the thickness dependence of quantities that are formally obtained as integrals over all (occupied) electronic states. In addition, it is instructive to monitor the effect of the finite thickness of the Pt slab on differential, state-resolved quantities. This can be achieved by inspecting the Bloch spectral function, which is defined via the imaginary part of the Green's function in the \mathbf{k} -space representation,³²

$$A^B(\mathbf{k}, E) = -\frac{1}{\pi} \text{Im}(\mathbf{k} | G(E) | \mathbf{k}). \quad (4)$$

Integration of $A^B(\mathbf{k}, E)$ over the full Brillouin zone results in the density of states

$$n(E) = \frac{1}{\Omega_{\text{BZ}}} \int_{\Omega_{\text{BZ}}} d^3k A^B(\mathbf{k}, E), \quad (5)$$

i.e., $A^B(\mathbf{k}, E)$ provides a \mathbf{k} -resolved measure for the density of states $n(E)$.

To demonstrate the dependence of the Bloch spectral function on the thickness of the Pt slab, we evaluated $A^B(\mathbf{k}, E)$ for a Co monolayer on Pt(111) with a bulklike structure, modeling the substrate by finite slabs of $n_{\text{Pt}}=9$ and $n_{\text{Pt}}=38$ layers and by a proper semi-infinite crystal. Diagrams depicting $A^B(\mathbf{k}, E)$ along the high symmetry lines $\bar{\Gamma}-\bar{K}-\bar{M}-\bar{\Gamma}$ in the two-dimensional Brillouin zone are shown in Fig. 4. For simplicity only the minority-spin states are shown. Local densities of minority-spin states $n_1(E)$ related to the Co atoms are also presented. As these are obtained by applying the integration [Eq. (5)] to the full surface Brillouin zone, they reflect also other states than those for which $A^B(\mathbf{k}, E)$ is displayed.

The bottom diagram of Fig. 4 illustrates how the energy bands of the Co monolayer (dark regions) are broadened due to hybridization with the states of the underlying semi-infinite Pt substrate (gray-shaded areas). For finite Pt slabs, however, the continuum of the Pt substrate states is replaced by discrete energy bands because of the quantum confinement caused the finite width of the slab. Considerable changes in $A^B(\mathbf{k}, E)$ thus follow (especially for thinner slab in the top graph). For the densities of states, the difference between finite slabs and semi-infinite crystal is much less pronounced, as the integration [Eq. (5)] averages over differences. We expect that the same would be true for other \mathbf{k} -integrated quantities.

B. Dependence of magnetic moments and the MAE on the concentration of adatoms

In theoretical studies, periodic nanostructures described by surface supercells are often used instead of the proper geometry of isolated adatoms so that band-structure methods formulated in reciprocal space can be used. To verify the robustness of this procedure, we calculate the magnetic properties of a sequence of Fe and Co surface superstructures on Pt(111), with different supercell sizes. The substrate is modeled by a slab of ten Pt layers throughout the sequence. The

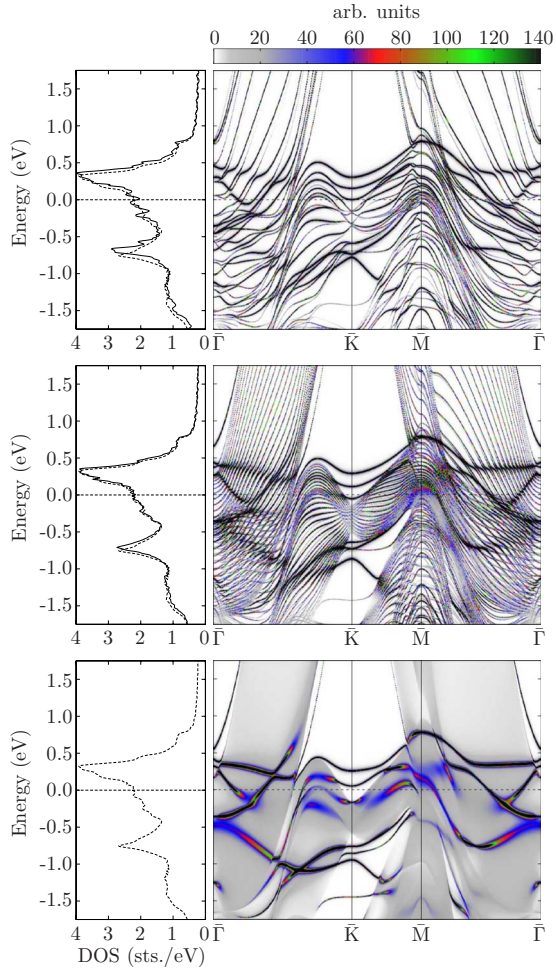


FIG. 4. (Color online) Minority-spin Bloch spectral functions $A^B(\mathbf{k}, E)$ at the Co sites for a Co monolayer on Pt(111), with bulk-like interlayer distances. The substrate is modeled by finite slabs of 9 and 38 layers (topmost and middle diagrams, respectively) and by a proper semi-infinite crystal (lowermost diagram). The color-coded scale of $A^B(\mathbf{k}, E)$ intensities is shown at the top. In the left panels, densities of states at the Co sites are displayed. In the case of finite slabs, the DOS for the semi-infinite crystal is also shown via dotted lines for comparison (topmost and middle diagrams).

results for μ_{spin} and μ_{orb} at Fe and Co atoms and for the MAE are shown in Fig. 5. One can see that the magnetic moments converge rapidly with the supercell dimension (even the least diluted $\sqrt{3} \times \sqrt{3}$ coverage yields similar results as adatoms). On the other hand, the MAE depends on the supercell dimensions quite strongly and in a nonmonotonic way. The relative change in the MAE when going from the largest supercell we explored ($\sqrt{7} \times \sqrt{7}$) to the adatom case can be as large as 50–100 %.

The MAE for surface superstructures thus considerably differs from the MAE for adatoms. Quantitative predictions concerning the MAE of adatoms cannot be made if the adatom is modeled by a superstructure with concentration of adatoms $\geq 10\%$.^{10,31} As concerns more diluted systems such as 4×4 or 5×5 supercells,^{5,6} the situation remains unclear (performing such calculations for $n_{\text{Pt}}=10$ would be computationally very expensive and thinner slabs are still in the oscillatory regime as concerns n_{Pt}).

The magnetic moments presented in Fig. 5 correspond to the magnetization perpendicular to the surface, $\mathbf{M}_{\parallel z}$. We performed also self-consistent calculations with in-plane magnetization, $\mathbf{M}_{\parallel x}$. We found that while μ_{orb} depends on the direction of \mathbf{M} considerably (variations are $\sim 20\text{--}40\%$), μ_{spin} practically does not change at all; the relative variations in μ_{spin} for Fe and Co atoms for any coverage or $z_{\text{Fe/Co-Pt}}$ distance are less than 1%. In this respect our results differ from those of Etz *et al.*⁴ who reported a larger anisotropy in μ_{spin} (about 3% for a Fe adatom and as much as 8% for a Co adatom).⁴ For μ_{spin} induced in the Pt slab, the variations caused by different \mathbf{M} orientations are a bit larger, about 5–15 %. This is consistent with earlier results of Blonski and Hafner.⁶

The MAE presented here concerns the difference $E_x - E_z$, with the x axis defined so that it corresponds to the horizontal direction in Fig. 1. We assume that similar results would be obtained if the in-plane magnetization was defined for any other azimuth angle. We tested this specifically for the Fe 2×2 supercell on Pt(111) with a semirelaxed geometry and found that $E_{\theta=0^\circ, \phi} - E_z$ varies between 0.495 and 0.560 meV if the azimuth angle ϕ is varied. The anisotropy in the xy plane is thus about ten times less than is the anisotropy between the in-plane and out-of-plane directions. For adsorbed clusters, however, the situation may be different.³³

The shape anisotropy is not the subject of our study, nevertheless, it should be mentioned that its contribution is about -0.09 meV for a Co monolayer and about -0.18 meV for a Fe monolayer (both for the bulklike and semirelaxed geometries). This means that for a Fe monolayer, this contribution can be significant because the magnetocrystalline MAE of a Fe monolayer is quite small. For more diluted coverages, the shape contribution to the MAE can be neglected: it is several times smaller than for a full monolayer and, on top of that, the magnetocrystalline MAE is much larger.

Contribution of the substrate

To understand the problem of the MAE in these systems, one needs more information about the role of the adatoms and of the substrate. However, energy is not an extensive quantity and so one cannot decompose the MAE uniquely into sums of contributions coming from individual parts. Assigning one part of the MAE to the adatom and another part to the substrate can be only intuitive and in principle ambiguous. We perform this assignment by analyzing contributions of individual sites to the total torque exerted on the system if the magnetization is tilted by 45° (cf. Sec. II). This approach is intuitively appealing because the individual terms we compare—torque moments exerted on atoms—correspond to real physical quantities (even though these moments are not independent).

To quantify the relative importance of the substrate, we evaluate the ratio of the torque exerted on all the Pt atoms τ_{Pt} to the torque exerted on Fe or Co atoms $\tau_{\text{Fe/Co}}$. The results are summarized in Table I. It follows from Table I that substrate contributions to the torque are typically not important,

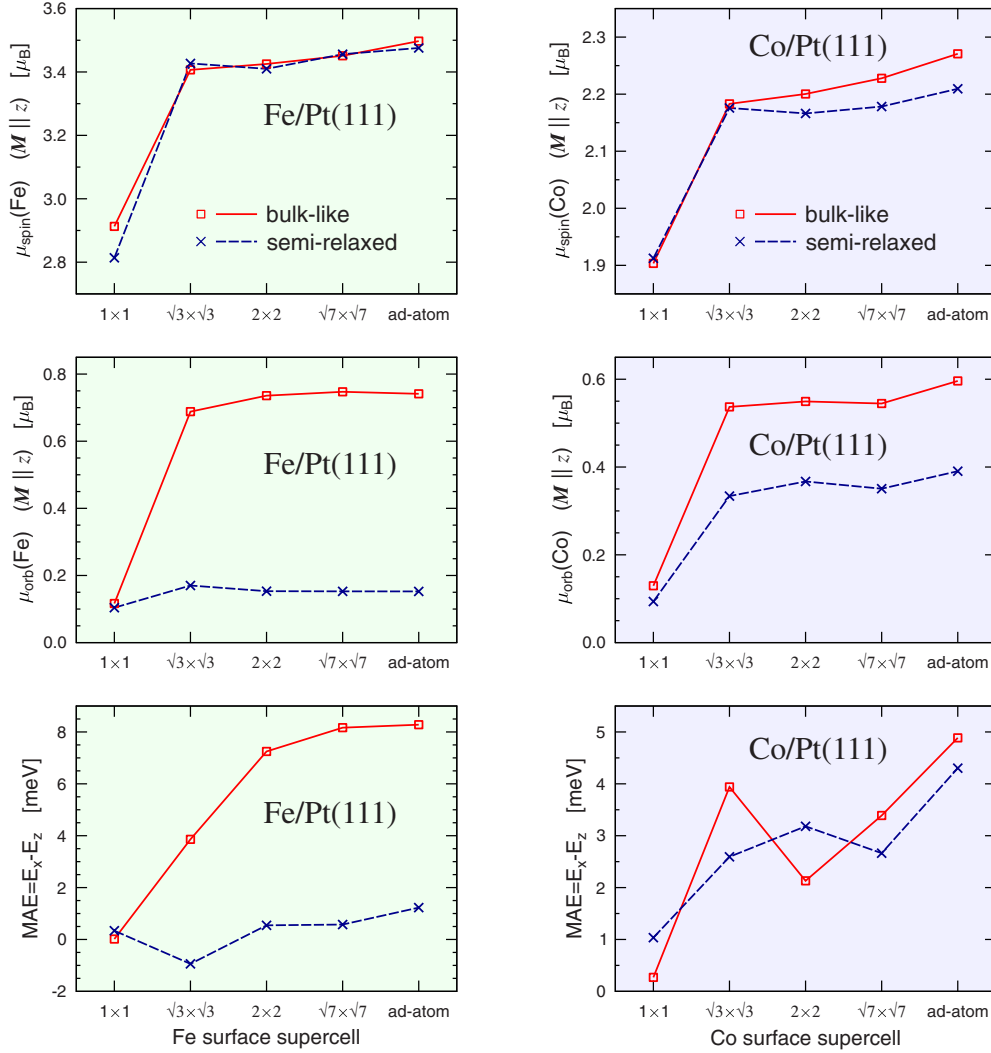


FIG. 5. (Color online) Calculated magnetic properties of Fe (left panels) and Co (right panels) surface supercells on Pt(111) with bulklike and semirelaxed structures. Magnetic moments obtained for magnetization perpendicular to the surface are shown in the upper panels (μ_{spin}) and in the middle panels (μ_{orb}). The lowermost panels display the MAE per Fe or Co atom. The surface superstructures are depicted in Fig. 1.

except for a complete monolayer coverage. The substrate contribution is larger for semirelaxed systems, where the Fe/Co-Pt distances are contracted with respect to the bulklike distances. For these semirelaxed systems, τ_{Pt} is more important in case of Fe adsorbates than in case of Co adsorbates.

In some respects, e.g., concerning the larger role of the substrate for monolayers than for adatoms, our results are similar to earlier findings of Moulas *et al.*² and Etz *et al.*⁴ (who based their scheme on comparing how different sites contribute to the difference of band energies). In other respects the results differ, as for instance in the case of adatoms, where the substrate contribution to the difference of the band energies obtained by Etz *et al.*⁴ is much larger than the substrate contribution to the total torque found in this work. The reason for this difference may be linked to the ambiguity of the splitting of the MAE into individual components. It should be emphasized, however, that the total sum over all the sites does not depend on whether we sum the torque or the differences in the band energy, as it was noted in Sec. II already.

TABLE I. The ratio of the substrate contribution τ_{Pt} to the total torque to the contributions of Fe/Co atoms $\tau_{\text{Fe/Co}}$ for Fe/Co surface superstructures. The first column indicates the coverage, the following two columns contain the ratio between the torque contributions for systems with bulklike interlayer distances, and the last two columns contain the same for systems with semirelaxed interlayer distances. A negative value means that the torque on Pt atoms has different orientation than the torque on Fe atoms.

	Bulklike		Semirelaxed	
	Fe	Co	Fe	Co
	$\tau_{\text{Pt}}/\tau_{\text{Fe}}$	$\tau_{\text{Pt}}/\tau_{\text{Co}}$	$\tau_{\text{Pt}}/\tau_{\text{Fe}}$	$\tau_{\text{Pt}}/\tau_{\text{Co}}$
1×1	-0.55	1.48	0.24	0.17
$\sqrt{3} \times \sqrt{3}$	-0.04	0.01	0.21	0.02
2×2	-0.01	0.00	0.12	0.05
$\sqrt{7} \times \sqrt{7}$	0.00	0.01	0.16	0.04
Adatom	0.00	0.00	0.04	0.02

TABLE II. Total μ_{spin} and μ_{orb} induced by Fe and Co adatoms in the Pt substrate, obtained if embedded clusters of 76 Pt atoms are employed. The first column identifies the adatom type and geometry, the second column contains induced μ_{spin} if SOC is neglected, and the third and fourth columns contain μ_{spin} and μ_{orb} for the substrate of SOC is included.

Adatom, geometry	Without SOC		Including SOC	
	μ_{spin} (μ_B)	μ_{spin} (μ_B)	μ_{spin} (μ_B)	μ_{orb} (μ_B)
Fe, bulklike	0.57	0.49	0.080	
Co, bulklike	0.52	0.43	0.079	
Fe, semirelaxed	0.79	0.70	0.131	
Co, semirelaxed	0.71	0.61	0.142	

To summarize the whole part (Sec. IV B), the MAE of surface superstructures differs considerably from the MAE of adatoms. Quantitative predictions thus cannot be made if the adatom is modeled by a superstructure with a concentration of adatoms that is larger than about 10%.^{10,31}

C. Comparison with other works

This work demonstrates that the MAE is very sensitive to the way the substrate is modeled and to the size of the supercell used to model the adatom coverage. Earlier works demonstrated that the MAE is very sensitive to interatomic distances (geometry relaxation).^{5,6} Comparing different calculations of the MAE thus can be strictly done only if the structures used in the calculations are really identical, which is usually not the case. The situation is different with magnetic moments of adatoms and adlayers because these are not so sensitive to the way the substrate is modeled. If we restrict ourselves to bulklike geometries, we find good agreement of our values of μ_{spin} and μ_{orb} at Fe and Co atoms with earlier calculations for a supported Fe monolayer,^{4,10} for a Fe adatom^{4,6} (though Ref. 6 reports a smaller value for μ_{orb}), for a supported Co monolayer,^{4,7} for a supported 2×2 Co surface supercell,³¹ and for a Co adatom.⁴⁻⁷

Concerning the magnetic moments induced in the Pt substrate, the agreement between different works is less good. The total μ_{spin} and μ_{orb} in the Pt substrate obtained by us for the case of Fe and Co adatoms is summarized in Table II. These values are much less than the moments obtained by Blonski and Hafner.⁶ The ratio $\mu_{\text{orb}}/\mu_{\text{spin}}$ is very similar in both works, on the other hand. Balashov *et al.*³ present only the total μ_{spin} which includes contributions both from the Fe and Co adatoms and from the Pt(111) substrate; their values are about 0.4 μ_B less than our values (for bulklike geometry). We can also make a partial comparison with Etz *et al.*:⁴ they present μ_{spin} induced at those Pt atoms which are nearest neighbors to the Fe/Co adatoms and their values are about 20% larger than our values.

Blonski and Hafner⁶ suggest that the disagreement between their values of induced moments and the values obtained by studies which employ the impurity Green's-function technique (Refs. 4 and 33 and this work) is caused

TABLE III. Dependence of the total μ_{spin} and total μ_{orb} induced in a Pt substrate by a Co adatom on the size of the embedded cluster. The semirelaxed geometry is used.

No. of Pt atoms	μ_{spin} (μ_B)	μ_{orb} (μ_B)
6	0.363	0.069
15	0.536	0.115
18	0.544	0.123
30	0.576	0.136
34	0.604	0.152
76	0.611	0.143
160	0.632	0.144
283	0.647	0.141

by a too small spacial extension of the induced polarization cloud in the latter studies. In principle, this might indeed be the case. Etz *et al.*⁴ allow electronic-structure relaxation at 30 Pt atoms (within four shells around the adatoms), the values shown in our Table II were obtained by allowing electronic-structure relaxation at 76 atoms. This may seem insufficient in the view of the fact that, e.g., for a Co impurity in bulk Pd, the polarization cloud includes up to thousand atoms.³⁴ The polarization cloud in bulk Pt, however, is much smaller.¹⁶ We verified that increasing our embedded cluster so that it contains as much as 283 Pt atoms does not lead to dramatic changes in the total μ_{spin} in the substrate (see Table III). The size of the embedded cluster thus cannot be the cause of the difference between our results and the results of Blonski and Hafner⁶ (who have got 125 Pt atoms in their supercell).

Another issue linked to the induced moments concerns the difference between scalar-relativistic and fully relativistic calculation. Blonski and Hafner⁶ found that switching on the SOC reduces the total μ_{spin} at Pt atoms from 4.83 to 3.32 μ_B for a Co adatom in an hcp position (for a relaxed geometry). A much smaller reduction was found for a Fe adatom in an fcc position (from 2.38 to 2.15 μ_B).⁶ Our calculations lead to a much smaller effect in the case of the Co adatom, as demonstrated by the values of the total induced μ_{spin} presented in Table II). If relative changes are considered, the difference between our results and the results of Blonski and Hafner⁶ is not that striking but still significant: we find that the inclusion of the SOC reduces the induced μ_{spin} by 11–16 % for both Fe and Co adatom alike while the reduction obtained by Blonski and Hafner⁶ is 9% for the Fe adatom and 31% for the Co adatom.

V. CONCLUSIONS

Finite thickness of the slab which represents the substrate and interaction between the adatoms affect calculated values of the MAE much more profoundly than they affect calculated values of magnetic moments. Reliable theoretical values for the MAE thus cannot be obtained if the substrate is represented by slab of less than 7–10 atomic layers or if the

surface supercell describing the adatoms is so small that the adatoms concentration is more than few percent.

The structural relaxation highlighted earlier is clearly very important (as it follows from this work as well). However, it is also necessary to properly account for the semi-infinite substrate and to make sure that the adatoms do not influence each other. Only if these conditions are guaranteed, reliable calculations of MAE can be performed.

ACKNOWLEDGMENTS

This work was supported by the Grant Agency of the Czech Republic within the Project No. 202/08/0106 and by the Deutsche Forschungsgemeinschaft within the Project No. Mi-1327/1. The research in the Institute of Physics, AS CR was supported by the Project No. AV0Z-10100521 of Academy of Sciences of the Czech Republic.

*sipr@fzu.cz; <http://www.fzu.cz/~sipr>

†hubert.ebert@cup.uni-muenchen.de

<http://ebert.cup.uni-muenchen.de>

- ¹P. Gambardella, S. Rusponi, M. Veronese, S. S. Dhesi, C. Grazioli, A. Dallmeyer, I. Cabria, R. Zeller, P. H. Dederichs, K. Kern, C. Carbone, and H. Brune, *Science* **300**, 1130 (2003).
- ²G. Moulas, A. Lehnert, S. Rusponi, J. Zabloudil, C. Etz, S. Ouazi, M. Etzkorn, P. Bencok, P. Gambardella, P. Weinberger, and H. Brune, *Phys. Rev. B* **78**, 214424 (2008).
- ³T. Balashov, T. Schuh, A. F. Takacs, A. Ernst, S. Ostanin, J. Henk, I. Mertig, P. Bruno, T. Miyamachi, S. Suga, and W. Wolfhekel, *Phys. Rev. Lett.* **102**, 257203 (2009).
- ⁴C. Etz, J. Zabloudil, P. Weinberger, and E. Y. Vedmedenko, *Phys. Rev. B* **77**, 184425 (2008).
- ⁵A. Mosca Conte, S. Fabris, and S. Baroni, *Phys. Rev. B* **78**, 014416 (2008).
- ⁶P. Błoński and J. Hafner, *J. Phys.: Condens. Matter* **21**, 426001 (2009).
- ⁷B. Lazarovits, L. Szunyogh, and P. Weinberger, *Phys. Rev. B* **67**, 024415 (2003).
- ⁸B. Nonas, I. Cabria, R. Zeller, P. H. Dederichs, T. Huhne, and H. Ebert, *Phys. Rev. Lett.* **86**, 2146 (2001).
- ⁹A. B. Shick, F. Maca, and A. I. Lichtenstein, *J. Appl. Phys.* **105**, 07C309 (2009).
- ¹⁰M. Tsujikawa, A. Hosokawa, and T. Oda, *J. Phys.: Condens. Matter* **19**, 365208 (2007).
- ¹¹J. G. Gay and R. Richter, *Phys. Rev. Lett.* **56**, 2728 (1986).
- ¹²I. V. Solovyev, P. H. Dederichs, and I. Mertig, *Phys. Rev. B* **52**, 13419 (1995).
- ¹³J. Vackar and A. Šimůnek, *Phys. Rev. B* **67**, 125113 (2003).
- ¹⁴J. P. Chou, H. Y. T. Chen, C. R. Hsing, C. M. Chang, C. Cheng, and C. M. Wei, *Phys. Rev. B* **80**, 165412 (2009).
- ¹⁵S. Chadov, J. Minar, M. I. Katsnelson, H. Ebert, D. Kodderitzsch, and A. I. Lichtenstein, *EPL* **82**, 37001 (2008).
- ¹⁶O. Šipr, J. Minar, S. Mankovsky, and H. Ebert, *Phys. Rev. B* **78**, 144403 (2008).
- ¹⁷A. B. Shick and O. N. Mryasov, *Phys. Rev. B* **67**, 172407 (2003).
- ¹⁸S. H. Vosko, L. Wilk, and M. Nusair, *Can. J. Phys.* **58**, 1200 (1980).
- ¹⁹H. Ebert, in *Electronic Structure and Physical Properties of Solids*, Lecture Notes in Physics Vol. 535, edited by H. Dreysse (Springer, Berlin, 2000), p. 191.
- ²⁰P. Weinberger, *Electron Scattering Theory for Ordered and Disordered Matter* (Oxford University Press, Oxford, 1990).
- ²¹R. Zeller, P. H. Dederichs, B. Ujfalussy, L. Szunyogh, and P. Weinberger, *Phys. Rev. B* **52**, 8807 (1995).
- ²²M. P. Lopez Sancho, J. M. Lopez Sancho, and J. Rubio, *J. Phys. F: Met. Phys.* **15**, 851 (1985).
- ²³J. Minar, S. Bornemann, O. Šipr, S. Polesya, and H. Ebert, *Appl. Phys. A: Mater. Sci. Process.* **82**, 139 (2006).
- ²⁴S. Bornemann, J. Minar, S. Polesya, S. Mankovsky, H. Ebert, and O. Šipr, *Phase Transitions* **78**, 701 (2005).
- ²⁵J. B. Staunton, L. Szunyogh, A. Buruzs, B. L. Gyorffy, S. Ostanin, and L. Udvardi, *Phys. Rev. B* **74**, 144411 (2006).
- ²⁶X. D. Wang, R. Q. Wu, D. S. Wang, and A. J. Freeman, *Phys. Rev. B* **54**, 61 (1996).
- ²⁷R. F. Sabiryanov, M. I. Larsson, K. J. Cho, W. D. Nix, and B. M. Clemens, *Phys. Rev. B* **67**, 125412 (2003).
- ²⁸B. Hardrat, A. Al-Zubi, P. Ferriani, S. Blugel, G. Bihlmayer, and S. Heinze, *Phys. Rev. B* **79**, 094411 (2009).
- ²⁹R. Wu, C. Li, and A. J. Freeman, *J. Magn. Magn. Mater.* **99**, 71 (1991).
- ³⁰F. Meier, K. von Bergmann, P. Ferriani, J. Wiebe, M. Bode, K. Hashimoto, S. Heinze, and R. Wiesendanger, *Phys. Rev. B* **74**, 195411 (2006).
- ³¹A. B. Shick and A. I. Lichtenstein, *J. Phys.: Condens. Matter* **20**, 015002 (2008).
- ³²J. S. Faulkner and G. M. Stocks, *Phys. Rev. B* **21**, 3222 (1980).
- ³³S. Bornemann, J. Minar, J. B. Staunton, J. Honolka, A. Enders, K. Kern, and H. Ebert, *Eur. Phys. J. D* **45**, 529 (2007).
- ³⁴R. Zeller, *Modell. Simul. Mater. Sci. Eng.* **1**, 553 (1993).